ControlMol: Adding Substruture Control To Molecule Diffusion Models

Zhengyang Qi[1*] , **Zijing Liu**[2] , **Jiying Zhang**[2] , **He Cao**[2] , **Yu Li**[2]

[1]University of Science and Technology of China
[2]International Digital Economy Academy(IDEA)

miloq@mail.ustc.edu.cn, {liuzijing, zhangjiying,caohe,liyu}@idea.edu.cn

Abstract

Designing new molecules is an important task in the field of pharmaceuticals. Due to the vast design space of molecules, generating molecules conditioned on a specific sub-structure relevant to a particular function or therapeutic target is a crucial task in computer-aided drug design. In this paper, we present ControlMol, which adds sub-structure control to molecule generation with diffusion models. Unlike previous methods which view this task as inpainting or conditional generation, we adopt the idea of ControlNet into conditional molecule generation and make adaptive adjustments to a pretrained diffusion model. We apply our method to both 2D and 3D molecule generation tasks. Conditioned on randomly partitioned sub-structure data, our method outperforms previous methods by generating more valid and diverse molecules. The method is easy to implement and can be quickly applied to a variety of pre-trained molecule generation models.

1 Introduction

Molecule generation has become a fundamental task in drug design. Traditional methods of molecule design often relied on intuition, trial and error, and the expertise of medicinal chemists. In recent years, diffusion models [Ho *et al.*, 2020], a promising class of generative models, have been applied to molecule generation. Meanwhile, a multitude of diffusion models [Hoogeboom *et al.*, 2022; Xu *et al.*, 2022; Jing *et al.*, 2022; Vignac *et al.*, 2023; Vignac *et al.*, 2022] automatically generating molecular geometries (i.e. 2D graphs or 3D point clouds) from scratch have been proposed.

The primary goal of molecular design is to propose novel molecules that satisfy desired properties. In the past few yeas, there have been many machine learning methods to address this problem [Kang and Cho, 2018; Yang *et al.*, 2023]. The diffusion-based generate-from-scratch methods can also easily be implemented to be conditioned on some predefined scalar properties [Hoogeboom *et al.*, 2022; Huang *et al.*, 2022]. However, they still suffer from the huge

space of diversity spaces. As in [Virshup *et al.*, 2013], the space of pharmacologically-relevant molecules is estimated to exceed 10^{60} structures. Searching in such space poses significant challenges for drug design. To reduce the size of the searching space, the strategy fragment-based drug design(FBDD) [Erlanson *et al.*, 2016] generates molecules from fragments. An important stage of drug design is Lead Optimization, which aims to optimize the favorable properties of compounds by changing part of their atoms [Hughes *et al.*, 2011]. Some diffusion methods [Torge *et al.*, 2023; Igashov *et al.*, 2022; Schneuing *et al.*, 2022]) also try to address this issue, they improve the de-novo molecule generation method by allowing it to receive 3D structure conditions. However, their focus is centered on some certain specific data, such as scaffold or linker data. We, on the other hand, aim to explore the possibility of conditioning on a wider and more diverse set of data, and study effective training methods.

DiffSBDD [Schneuing *et al.*, 2022] treats this molecule generation task conditioned on the structure context as an inpainting [Song *et al.*, 2020; Lugmayr *et al.*, 2022]task in images, this inspired us to draw technology from image processing. Recently, a lot of non-invasive tuning methods [Li *et al.*, 2023; Mou *et al.*, 2023; Zhang *et al.*, 2023] have achieved surprising results in image control, instead of finetuning the origin model, they train an additional auxiliary module to change the features transferring between layers. Compared to traditional condition generation methods, these methods are more flexible and efficient. Among these studies, ControlNet [Zhang *et al.*, 2023] has garnered more attention for its simple implementation and powerful effects, it addresses the lack of fine control in image generation and the redundancy and complexity of prompts combinations, bringing more diverse conditional control to the generative model. Although similar idea has expanded from images to other areas like voice and video, there is still a lack of such tries in molecule science.

In this work, we introduce ControlMol, a substructure conditional diffusion model architecture that exploits ControlNet [Zhang *et al.*, 2023]. We will use the EDM [Hoogeboom *et al.*, 2022], an equivariant diffusion model for molecule generation to introduce our method. ControlMol receives a molecule substructure as a condition and generates conformers with this context. Compared to previous methods, ControlMol uses readily available data and can generate more

---

[*]Work done during an internship at IDEA.

valid molecules.

Our contributions can be summarized as follows. We introduce the concept of ControlNet [Zhang *et al.*, 2023] into molecule generation, enabling an unconditional diffusion model to accept substructure control. We first focus on the task of 3D molecular conformation generation and then we further verify its effectiveness in 2D molecule graph generation. ControlMol method naturally utilizes the base model's performance and generates high-quality molecules. Interestingly, we find that the ControlMol model can accept various sub-structure control even though it is trained on the dataset of random subgraph partitioning, which indicates that ControlMol learns a more generalized distribution.

2 Related Work

Diffusion Model And Controllable Generation Denoising Diffusion Probabilistic model(DDPM) [Ho *et al.*, 2020] is a powerful class of generative model used to learn complex probability distributions. Diffusion models have shown powerful capabilities in processing image-like data when their underlying neural backbone is implemented as a UNets [Ronneberger *et al.*, 2015]. After achieving success in image generation, diffusion models are quickly applied to synthesize text, speech, and other data. Compared to unconditional generation, controllable generation is more attractive. Existing works use classifier guided [Dhariwal and Nichol, 2021] and classifier free [Ho, 2022] method to generate images belonging to some class. Stable diffusion [Rombach *et al.*, 2021] effectively employs text prompts as guidance for diffusion models, enabling them to generate images that adhere to specific textual contexts, they utilize a pre-trained text encoder to get text embeddings and map the embedding to cross-attention layers to guide the hidden features in Unet layers. Later, a series of non-invasive fine-tuning methods, represented by GLIGEN [Li *et al.*, 2023], ControlNet [Zhang *et al.*, 2023], and T2IAdapter [Mou *et al.*, 2023], emerged. They enable the model to accept more diverse conditional controls by adding and fine-tuning additional modules.

Molecule Generation Deep generative models exhibit their effectiveness in modeling molecular data. Recently, generating molecules in 3D space has gained a lot of attention. G-Schnet [Gebauer *et al.*, 2019] employs an auto-regressive process equipped with Schnet [Schütt *et al.*, 2017]in which atoms and bonds are sampled iteratively. These years, inspired by the success of diffusion models [Ho *et al.*, 2020], several recent works proposed denoising diffusion models for molecular data in 3D. GeoDiff [Xu *et al.*, 2022], TorsionalDiffusion [Jing *et al.*, 2022]condition the model on the adjacency matrix of the molecular graph. Equivirant Diffusion Model(EDM) [Hoogeboom *et al.*, 2022] generates 3D molecules from scratch. MDM [Huang *et al.*, 2022] encodes the interatomic relations between atoms, further improves the validness and diversity of molecular generation. MiDi [Vignac *et al.*, 2023] offers an end-to-end differentiable approach that streamlines the molecule generation process, which can generate the 3D conformation and 2D graph of a molecule simultaneously.

Substructure Based Molecule Generation Difflinker [Igashov *et al.*, 2022] based on EDM [Hoogeboom *et al.*, 2022], is the first work trying to adding 3D molecule control to molecule diffusion models. It concentrates on the linker design task, given two or several fragments, it generates atoms that can link each part. DiffHopp [Torge *et al.*, 2023] is designed for scaffold hopping task [Böhm *et al.*, 2004] with a similar method to Difflinker, one of the differences between the two tasks is that scaffold hopping typically redesigns the majority of a molecule, while the linker part is minor. DiffSBDD [Schneuing *et al.*, 2022] is a diffusion model for pocket-conditioned ligand generation. It adopts the method of Difflinker to deal with the protein pocket condition, while for ligand context, it treats this as an inpainting task, they diffuse the fixed atoms at each step and use it to replace the noise corresponding to fixed nodes.

3 PRELIMINARIES

3.1 Diffusion And Controllable Diffusion

Diffusion Model The diffusion model defines two processes, *diffusion process* and *reverse process*.

At a timestep $t = 0, \ldots, T$, the diffusion process distorts a data point **x**, mapping it to noise z_t.

$$q(z_t|x) = \mathcal{N}(z_t|\alpha_t x_t, \sigma_t^2 I), \qquad (1)$$

where $\alpha_t \in \mathbb{R}^+$ controls how much signal is retained and $\sigma_t \in \mathbb{R}^+$ controls how much noise is added. This diffusion process is Markov and can be equivalently written with transition distributions as:

$$q(z_t|z_s) = \mathcal{N}(z_t|\alpha_{t|s}z_s, \ \sigma_{t|s}^2 I), \qquad (2)$$

for any $t > s$ with $\alpha_{t|s} = \alpha_t/\alpha_s$ and $\sigma_{t|s}^2 = \sigma_t^2 - \alpha_{t|s}^2\sigma_s^2$. The entire noising process is then written as:

$$q(z_0, z_1, \ldots, z_T|x) = q(z_0|x) \prod_{t=1}^{T} q(z_t|z_{t-1}). \quad (3)$$

And the reverse of the diffusion process, *the true denoising process*, also admits a closed-form solution when conditioned on x:

$$q(z_s|x, z_t) = N(z_s|\mu_{t \to s}(x, z_t), \sigma_{t \to s}^2 I), \qquad (4)$$

where the definitions for $\mu_{t \to s}(x, z_t)$ and $\sigma_{t \to s}$ can be analytically obtained as

$$\mu_{t \to s}(x, z_t) = \frac{\alpha_{t|s}\sigma_s^2}{\sigma_t^2}z_t + \frac{\alpha_s\sigma_{t|s}^2}{\sigma_t^2}x \quad \text{and} \quad \sigma_{t \to s} = \frac{\sigma_{t|s}\sigma_s}{\sigma_t}.$$

The reverse process learns to invert this trajectory having the data point x unknown. The generative transition distribution is defined as:

$$p(z_s|z_t) = \mathcal{N}(z_s|\mu_{t \to s}(\hat{x}, z_t), \sigma_{t \to s}^2 I). \qquad (5)$$

where $\hat{x}$ is an approximation of the data point **x** computed by a neural network φ, [Ho *et al.*, 2020] empirically shows that it works better to predict the Gaussian noise, if $z_t = \alpha_t x + \sigma_t$, then the neural network φ outputs $\epsilon, \hat{\epsilon} = \phi(z_t, t)$, so that :

$$\hat{x} = (1/\alpha_t) \, z_t - (\sigma_t/\alpha_t) \, \hat{\epsilon} \qquad (6)$$

The neural network is trained to maximize an evidence lower bound to the likelihood of the data under the model. The training objective can be simplied as $\mathcal{L}(t) = ||\epsilon - \hat{\epsilon}_t||^2$.
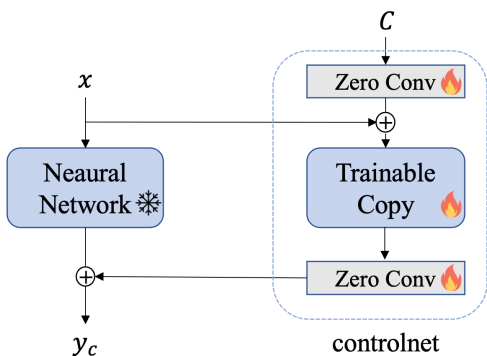
Figure 1: ControlNet injects conditions into neural network, where x denotes the original input and C denotes condition input.

Adding Control To Diffusion Models ControlNet [Zhang *et al.*, 2023] successfully combines the visual prompts without retraining the entire diffusion model. We use Control-Net represents the method and controlnet represents the replicated network. Specifically, as Figure 1 shows, it freezes the pre-trained model and reuses the deep and robust encoding layers as a robust backbone(trainable copy) for acquiring diverse conditional controls. The trainable copy and original model are linked by zero convolution layers, progressively growing parameters from zero, ensuring a stable fine-tuning process. This approach allows us to control diffusion models with learned conditions. In ControlNet, The denoising process takes input from both text and the outputs of the controlnet, so that the neural network φ outputs:

$$\hat{\epsilon} = \epsilon(z_t, \mathcal{T}, \text{controlnet}(z_t + \mathcal{E}_{2D})), \qquad (7)$$

where $\mathcal{T}$ is the text prompt, $\mathcal{E}_{2D}$ is the 2D visual prompts.

3.2 Diffusion For Molecules

Molecule Representation We inherit the settings of EDM [Hoogeboom *et al.*, 2022]. A molecular with N atoms is represented as geometric graph $\mathcal{G} = \{x, h\}$ with coordinates $x \in \mathbb{R}^{N \times 3}$ and node features $h \in \mathbb{R}^{N \times d}$. In particular, bond types are not predicted by diffusion models directly, but are given by the distance between pairs of atoms and the atom types [Satorras *et al.*, 2021a], so there is no symbol definition for edge attributes here.

Categorical Features Diffusion models typically operate on continuous data, such as images, voice, or atomic coordinates, while atom types are discrete. [Hoogeboom *et al.*, 2021] introduces discrete diffusion to handle categorical data. There exist such ideas in 2D molecule graph generation [Vignac *et al.*, 2022]. While in many 3D molecule diffusion works including EDM [Hoogeboom *et al.*, 2022], they lift the atom types to a continuous space: considering a one-hot encoding of the discrete variables, and adding Gaussian noise on top of it.

Network Architecture Diffusion model essentially uses Unets [Ronneberger *et al.*, 2015] as their neural network architecture in image generation. Due to different data types, many works([Hoogeboom *et al.*, 2022; Igashov *et al.*, 2022;

Schneuing *et al.*, 2022]) use E(n) Equivariant Graph Neural Networks(EGNNs)[Satorras *et al.*, 2021b] as their base model. In EDM's setting, EGNN consists of the composition of Equivariant Graph Convolutional Layers. $x^{l+1}, h^{l+1} = \text{EGCL}[x^l, h^l]$ which are defined as:

$$\text{m}_{ij} = \phi_e\left(h_i^l, h_j^l, d_{ij}^2\right), \ h_i^{l+1} = \phi_h(h_i^l, \sum_{j \neq i} \text{m}_{ij}),$$

$$x_i^{l+1} = x_i^l + \sum_{j \neq i} \frac{x_i^l - x_j^l}{d_{ij} + 1} \phi_x\left(h_i^l, h_j^l, d_{ij}^2\right), \qquad (8)$$

where l indexes the layer, $d_{ij} = \|x_i^l - x_j^l\|_2$ and ϕ_e, ϕ_h,ϕ_x are all learnable functions parameterized by fully connected neural networks.

At time t, EDM predicts noise $\hat{\epsilon}$ includes coordinate and feature components: $\hat{\epsilon} = [\hat{\epsilon}^x, \hat{\epsilon}^h]$. To make the network φ invariant to translations, the initial coordinates from the coordinate component of the predicted noise are subtracted:

$$\hat{\epsilon} = [\hat{\epsilon}^x, \hat{\epsilon}^h] = \varphi(z_t, t) = \text{EGNN}(z_t, t) - [z_t^x, 0]. \qquad (9)$$

(For more details on the network structure, we refer the reader to [Hoogeboom *et al.*, 2022]).

3.3 Inpainting Method

The diffusion model itself has the capacity for "inpainting" missing parts. As shown in DDPM [Ho *et al.*, 2020], the diffusion model can naturally recover the missing patches of images. Repaint [Lugmayr *et al.*, 2022] further improves the inpainting method, so that the model can recover the missing parts more harmonizing in a non-training way. As in DiffS-BDD [Schneuing *et al.*, 2022], it's natural and possible to view this substructure-based generation as an inpainting task using a model trained on de-novo molecule generation. Formally, given a known z_0, a current z_t and a mask indicating the known parts m, we can define

$$z_{t-1}^{\text{known}} \sim \mathcal{N}(\sqrt{\bar{\alpha}_{t-1}} z_0, (1 - \bar{\alpha}_{t-1})I) \qquad (10)$$

$$z_{t-1}^{\text{unknown}} \sim \mathcal{N}(\mu_\theta(z_t, t), \Sigma_\theta(z_t, t)) \qquad (11)$$

$$z_{t-1} = m \odot z_{t-1}^{\text{known}} + (1 - m) \odot z_{t-1}^{\text{unknown}} \qquad (12)$$

Repaint [Lugmayr *et al.*, 2022] notes that directly applying the method can lead to locally harmonized results that struggle to incorporate the global context. To compensate this, they use resampling, after getting z_{t-1} in Equation 12, they add noise to z_t again and repeat the complete process several times:

$$z_t \sim \mathcal{N}(\sqrt{\alpha_{t-1}} z_{t-1}, (1 - \alpha_{t-1})I) \qquad (13)$$

Following this way, we implement Repainti method (repeat for i times) in our experiment.

4 Method

In this section, we introduce ControlMol, a unified substructure-conditioned diffusion model for molecules. Additionally, by selecting an appropriate base model and properly setting, we can also keep the E(3)-equivariant property of the base model. In Section 4.1, we introduce the architecture of our model, explain our motivation and show how we
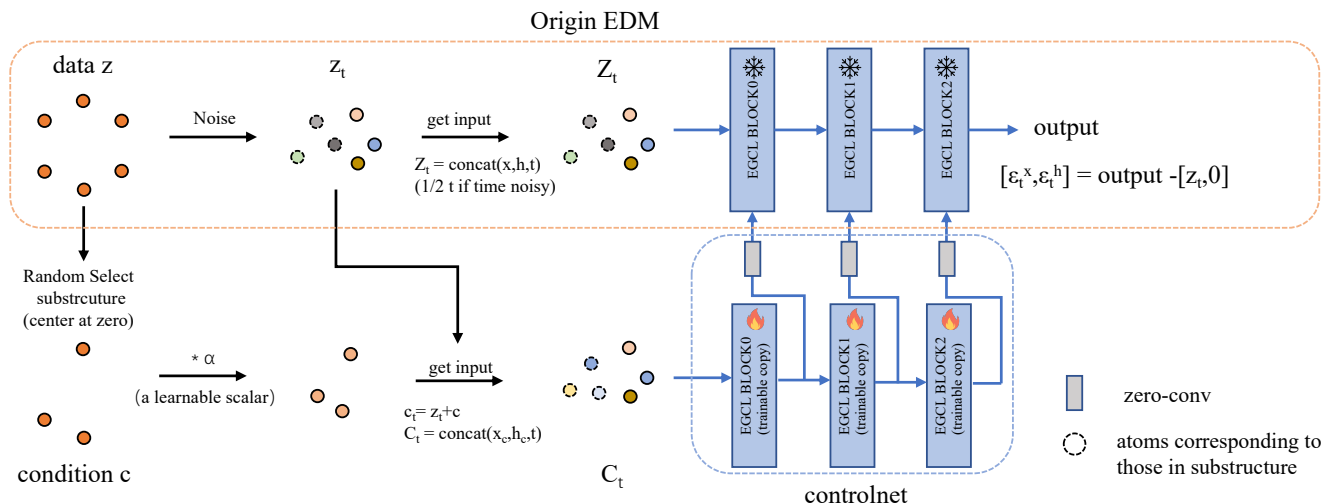
Figure 2: The overall architecture of ControlMol. The color of the node represents its node feature. After adding c, atoms corresponding to those in substructure in C_t are more similar to the origin substructure both in terms of their position and node feature compared to Z_t, this will implicitly provide conditions to the model.

get inspiration from ControlNet [Zhang *et al.*, 2023] on this problem and adapt it to non-Unets architecture. We discuss the details of the model and the equivariance requirements in Section 4.2.

4.1 ControlMol

We use EDM[Hoogeboom *et al.*, 2022] as our base model to introduce how to add 3D-substructure control to it. An overview of our method is presented in Figure 2.

EDM is an Equivariant diffusion model for 3D molecule generation. As in Equation 8, atom coordinates and node features influence and update each other. Additionally, the molecule should satisfy the correct valence relationship, it's more difficult to achieve good performance using a simple inpainting method.

Due to the distinctive architecture of the EGNN network, conditioning on a 3D structure can not be straightforwardly accomplished, as was previously done in EDM when conditioning on a desired property, by directly concat the property c and node feature h. Therefore, We try to utilize Control-Net [Zhang *et al.*, 2023] to achieve this goal. While original ControlNet is designed for Unets [Ronneberger *et al.*, 2015], which copies all encoders in stable diffusion [Rombach *et al.*, 2021] and passes the output to the decoder through zero-conv. Unlike Unets, EGNN consists of EGCL blocks, not encoder or decoder, and there are no explicit residual connections between its layers. For these reasons, as in Figure 2, we choose to replicate all layers of the primary network and introduce control mechanisms at each layer. In the Experiment section, we will show the correctness and efficacy of this configuration. In this way, The EGCL update process in Equation 8, after getting the update by EGCL block, $\boldsymbol{x}_i^{l+1}, \boldsymbol{h}_i^{l+1}$ get extra

update from ControlNet :

$$
\boldsymbol{x}_i^{l+1} = \boldsymbol{x}_i^{l+1} + \text{zeroconv}(\Delta control\_\boldsymbol{x}_i^{l+1})
$$
$$
\boldsymbol{h}_i^{l+1} = \boldsymbol{h}_i^{l+1} + \text{zeroconv}(control\_\boldsymbol{h}_i^{l+1}), \quad (14)
$$

where $control$ prefix represents the features in controlnet, and $\Delta control\_\boldsymbol{x}_i^{l+1} := control\_\boldsymbol{x}_i^{l+1} - control\_\boldsymbol{x}_i^l$ denotes the updated $\boldsymbol{x}$ in controlnet.

4.2 Model Details

Zero-conv The zero convolutions can be a unique type of connection layer that progressively grows from zeros to optimized parameters in a learned way so that it can stabilize the convergence of the model. Zero-conv in ControlNet[Zhang *et al.*, 2023] is a 1×1 convolution layer with both weight and bias initialized with zeros. In our work, we adopt the name "zero-conv". Due to the different data types, we choose one-layer Linear with weight and bias initialized with zero and learnable scalar initialized zero as our zero-conv. Learnable scalar can keep the E(3)-equivariant property of EDM. However, by experimental comparison, we found that choosing Linear as the zero-conv can accelerate the convergence of the model and enhance the control effectiveness.

Get Condition (sub-structure selection) For each data-point, we select a random proportion of atoms to be the 3D-context u. In practice, the proportion can also be set as a hyper-parameter. The reason for using a random sub-structure as a condition instead of selecting some specific pre-defined sub-structure data is that we expect the model to learn generalized distribution so that it can handle unseen sub-structures. For each datapoint, we sample a proportion $p \sim U(0, 1)$ and each atom is selected in sub-structure with this probability. Then we set the center of mass of u to be zero. In particular, we do not employ an additional encoder
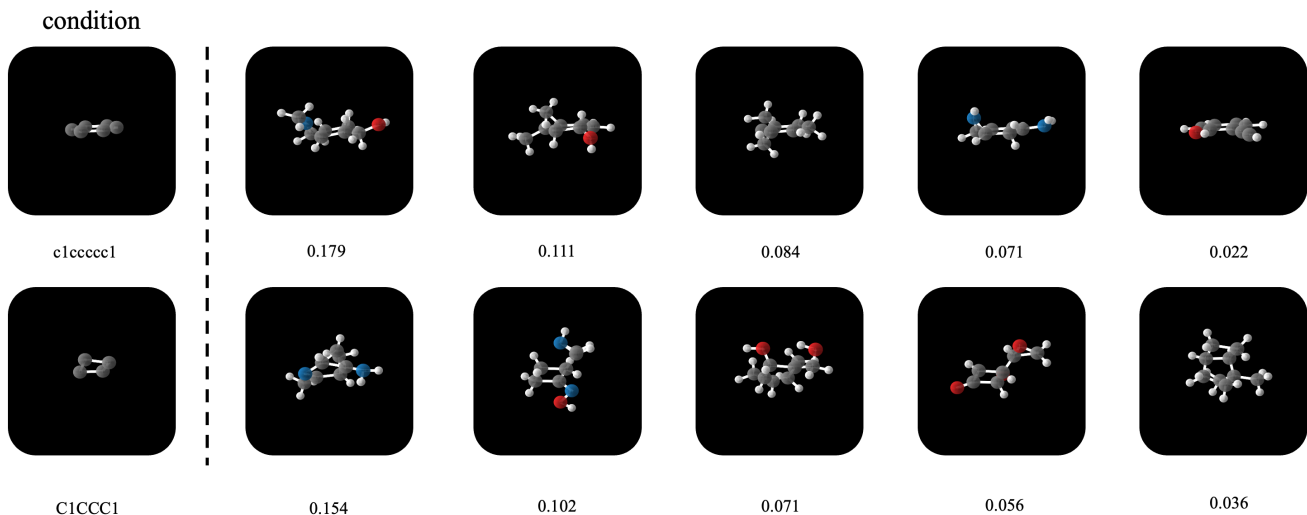
Figure 3: Samples conditioned on "c1ccccc1" and "C1CCC1", we use RDkit to generate their conformer from smiles and sample condition on it. The number behind the figure is the **RMSD** between samples with the conditioned conformer (structure on the left).

for feature extraction and instead directly feed it into controlnet. The input to controlnet(EGCL Block0(trainable copy) in Figure 2) at time t is:

$$h = h_t + \text{zeroconv}(sub\_h)$$
$$x = x_t + \text{zeroconv}(sub\_x) \qquad (15)$$

where sub prefix represents the features in substructure. Here we choose scalar as zero-conv to preserve the relative positional and type information.

Time Noisy   By experimentation, We observed that employing the ControlNet methodology in a straightforward way to an unconditional model is hard to train (difficulty in convergence or slow convergence rate). We reason that a well-trained model can estimate the data distribution effectively by itself, it may tend to overlook the information from additional modules. ControlNet [Zhang *et al.*, 2023] randomly replaces 50% text prompts with empty strings to facilitate learning from the condition. We need to find a method to enhance the learning of conditions for unconditional diffusion model. In this case, inspired by emuEdit [Sheynin *et al.*, 2023], which adds task embedding to time-embeddings to facilitate learning for different edit tasks, we try to drop some time information to relax the module capacity. Specifically, In EDM's setting, it concats node feature h and time t to add time information. At time t, we treat the input as follows (both in training and sampling):

$$h = \text{concat}(h_{\text{feature}}, t/2) \text{ (in main network)}$$
$$h = \text{concat}(h_{\text{feature}}, t) \quad \text{ (in controlnet)} \qquad (16)$$

The proposed time noisy technique is simple and efficient. It is based on the following intuition, T2IAdapter [Mou *et al.*, 2023] shows that the main of the generation results is determined in the early sampling stage. So, when t is large, we introduce a relatively significant bias to t, allowing the model to relearn the data distribution based on the condition. Therefore, the loss descends more steadily, reducing instances of training instability.

Algorithm 1 Training

Input: Datapoint x, pretrained neural network φ
controlnet $\varphi' = \text{copy}(\varphi)$
Sample $t \sim \mathcal{U}(0, \ldots, T)$, $\epsilon_t \sim \mathcal{N}(0, \mathbf{I})$, $p \sim \mathcal{U}(0, 1)$
Sample context u with probability p, center it at zero
$z_t \leftarrow \alpha_t x + \sigma_t \epsilon_t$
$c \leftarrow \alpha \cdot \mu$ (α reprents learnable scalar)
$c_t \leftarrow z_t + c$
$\hat{\epsilon}_t \leftarrow \varphi(z_t, \varphi'(c_t, t), t/2)$
Minimize $\|\epsilon - \hat{\epsilon}_t\|^2$

Algorithm 2 Sampling

Input: context u, neural network φ, controlnet φ'
Center context u at zero
Sample $z_T \sim \mathcal{N}(0, \mathbf{I})$
for t in T, $T - 1$, $\ldots$ 1:
    Sample $\epsilon_t \sim \mathcal{N}(0, \mathbf{I})$
    $c \leftarrow \alpha \cdot \mu$
    $c_t \leftarrow z_t + c$
    $\hat{\epsilon}_t \leftarrow \varphi(z_t, \varphi'(c_t, t), t/2)$
    $z_{t-1} \leftarrow (1/\alpha_{t|s}) \cdot z_t - \sigma_{t|s}^2/(\alpha_{t|s}\sigma_t) \cdot \hat{\epsilon}_t + \sigma_{t \rightarrow s} \cdot \epsilon$
end for
Sample $x \sim p(x|z_0, u)$

4.3   Equivariance

With the proper settings, ControlMol can keep the equivariant property of the EDM. Following the Proposition 1 in Difflinker [Igashov *et al.*, 2022], we have

Theorem 1. *u is the corresponding context of the data point x, a prior noise distribution $p(z_T|u) = \mathcal{N}(z_T; f(u), I)$, If f is O(3)-equivariant and φ is equivariant to joint O(3)-transformations of z_t and u, then $p(z_0|u)$ is O(3)-equivariant.*

In this work, u is the 3D-substructure, and φ is the whole model including the base model and controlnet. The features h are invariant to group transformations, for fea-

Methods	substructure	QM9(without H)				QM9(with H)			
		% h_success ↑	RMSD ↓	% Valid ↑	% Unique over Valid ↑	% h_success ↑	RMSD ↓	% Valid ↑	% Unique over Valid ↑
EDM-origin	-	-	-	97.5	94.3	-	-	91.9	90.7
Inpainting	C1CC1	100	0	6.8	100	100	0	1.2	100
	C1CCC1	100	0	7.7	97.4	100	0	1	100
	c1ccccc1	100	0	0.9	11.1	100	0	0	-
Difflinker	C1CC1	100	0	78.9	83.3	-	-	-	-
	C1CCC1	100	0	79.3	67.2	-	-	-	-
	c1ccccc1	100	0	49.9	0.2	-	-	-	-
ControlMol	C1CC1	94.2	0.164	**93.6**	99.4	90.2	0.111	**74.5**	100
	C1CCC1	96.4	0.071	**93.2**	99.0	89.6	0.088	**82.4**	99.7
	c1ccccc1	97.9	0.099	**94.9**	75.5	75.6	0.085	**75.9**	95.3

Table 1: The comparison over 1000 molecules of ControlMol and other baseline models on each conditional generation task. Three specific cyclic structures are chosen to show comparison results. EDM-Origin is the unconditioned base model we use. "-" in Difflinker means that it can not converge.

tures x, when we choose a E(3)-equivariant zero-conv such as a learnable scalar. The input in controlnet in Equation 15 is equivariant to joint O(3)-transformations of z_t and u, the controlnet architecture is also the EGCL, which make $\text{zeroconv}(\Delta control\_x_i^{l+1})$ in Equation 14 equivairant to input, so that the model φ is equivariant to joint O(3)-transformations of z_t and u. To make the model additionally translation invariant, we follow the same setting in Difflinker, center the context u at the center of mass zero and sample z_t from $\mathcal{N}(0, I)$.

5 Experiment

5.1 Experiments on EDM

Datasets We consider QM9 dataset. QM9 contains up to 9 atoms (29 atoms including hydrogens) and we use the same train/val/test partitions in EDM, which consists of 100k/18k/13k samples respectively for each partition.

Metrics We measure the validity, uniqueness of the samples. Same in the EDM [Hoogeboom *et al.*, 2022], we don't report the novelty. Additionally, to evaluate position control effectiveness, we estimate the Root Mean Squared Deviation (RMSD) between the generated and real sub-structure coordinates, and for node type control, we use h_success(samples which have the right substructure node type / sample number) to measure the proportion of the generated samples that have the correct node type of the context.

Baselines We compare our method with the inpainting-like method in DiffSBDD [Schneuing *et al.*, 2022] and we also incorporate the Repaint [Lugmayr *et al.*, 2022] method. Further, we train Difflinker [Igashov *et al.*, 2022] in randomly selected data(same as training ControlMol) instead of the fragment-linker data to be another baseline.

Results In Table 1. We report the performances of all the models in terms of four metrics. All methods share the same architecture of EDM [Hoogeboom *et al.*, 2022]. From Table 1, we can see that the proposed ControlMol outperforms all the previous baseline methods.

However, ControlMol generates all atoms while Difflinker only generates atoms excluding those in the sub-structure, so the structures in the samples may deviate slightly from those

in the conditions and this deviation is assessed by RMSD. It's worth noting that the RMSD in Table 1 is the average of all samples, people can freely define a threshold to filter the desired molecules. In Figure 3, we show some samples with conditioned sub-structure and their RMSD.

Inpainting methods perform poorly in all cases, even with the extra implementation of Repaint, it doesn't improve its performance, so we don't list its performance additionally in the table. Difflinker can work in QM9 without H, but its performance sharply declines on "c1ccccc1". Difflinker even can't generate any valid molecules in QM9 with H. We believe it is due to the training data. "c1ccccc1" is rare in QM9 and due to randomly selecting sub-structure, it's hard for the model to see similar data in training data. The maximum number of atoms in QM9 is 29 when including Hydrogens, the data distribution with randomly selected substructures is more diverse, which makes the model hard to learn. Benefiting from the frozen parameters, ControlMol can work well in these cases, generating high ratio valid molecules.

Experiments	epochs	% h_success ↑	RMSD ↓
no_tn_lr4	100	0	1.05
	200	1	0.8932
	300	1	0.9086
no_tn_lr5	100	1	0.9272
	200	19	0.5644
	300	29	0.3911

Table 2: The control performance for "c1ccccc1" for no_tn in Figure 4 (a)

Ablation study of timenoisy and zero-conv To test the effect of the "time noisy" and the different performance for zero-conv, we conduct ablation experiments in QM9 with H.

For time noisy, in Figure 4 (a), at the same hyperparameter settings, ControlMol with tn can converge to a lower loss at a faster rate. Figure 4 (b) shows that ControlMol with tn can achieve an acceptable control performance after epoch 120 (the EDM baseline we use is trained for 1100 epochs). In Table 2, without tn, even after 300 epochs, the control performance is still poor, we have conducted more experiments with different hyperparameters and obtained similar conclu-
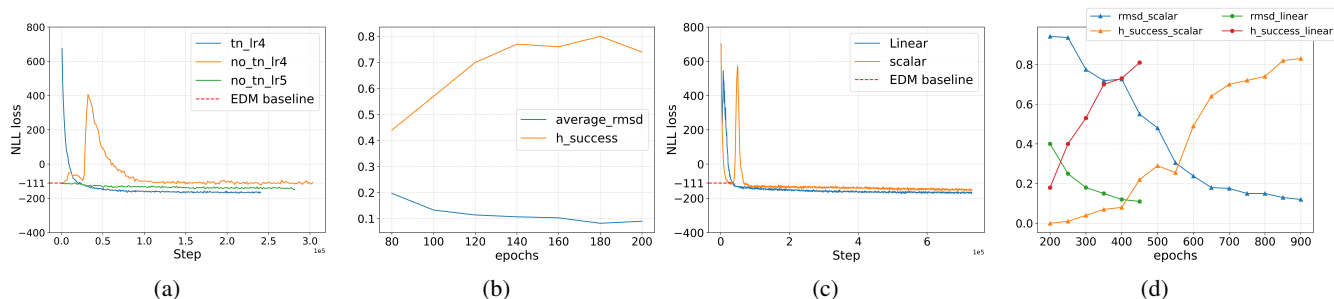
Figure 4: Ablation study of timenoisy and zero-conv. We choose "c1ccccc1" to evaluate the control performance in these experiments. (a) The loss curve for tn(time noisy) and no tn. lr4 notes that the learning rate is 1e-4 and lr5 is 1e-5. (b) The control performance for tn_lr4. (c) The loss curve for Linear and scalar (d) The control performance for Linear and scalar.

sions. Although the model without tn can improve performance with more epochs, it requires more costs for training.

For zero-conv, as in Figure 4 (c) and (d), the model with Linear can get a faster convergence and a better control performance in the same training epoch. The reason for different performances between Linear in Figure 4 (d) and in Figure 4 (b) is that we did experiments about zero-conv earlier when we use the substructure proportion $p \sim U(0.2, 0.5)$

5.2 Experiments for 2D control

To verify ControlMol's effectiveness, we conduct extra experiments in Digress [Vignac *et al.*, 2022] and MiDi [Vignac *et al.*, 2023]. Digress utilizes the discrete diffusion to generate 2D graph, its neuron network is graph transformer [Dwivedi and Bresson, 2020]. Based on Digress, MiDi further leverages the EGNN [Satorras *et al.*, 2021b] architecture to achieve the unified generation of 2D and 3D molecules.

For Digress, we test our method in QM9 and MOSES [Polykovskiy *et al.*, 2018] both without H. As shown in Table 3 and 4, our method outperforms Inpainting and Repaint method, especially in MOSES, which indicates our method can work better in larger datasets. However, we observe that "c1ccccc1" is a bad case for ControlMol in QM9, we speculate that the reason is that aromatic bond data is excessively sparse in QM9, so we test the performance on "C1CCCCC1", where the only difference between "c1ccccc1" and "C1CCCCC1" is their bond. Results show ControlMol can work successfully for "C1CCCCC1", so our method may still require some extra data augmentation methods in the future. For MiDi's experiments, We will show some visual results in Appendix **??**.

Although the Repaint method can get more valid molecules compared with Inpainting, it needs extra inference processes, which leads to an increase in sampling time. In our experiment on 2D control in MOSES, in table 4, the average sampling time per sample for Inpainting, Repaint5, Repaint20, and ControlMol are 1.13s, 7.54s, 27.7s, 1.57s (test on the A100 GPU).

6 Conclusion

We presented ControlMol, a method for adding 3D-structure control to diffusion models. ControlMol can generate more

Method	substructure	% condition ↑	% Relaxed Valid ↑	% Unique over valid ↑	% connectivity ↑
Digress-Origin	-	-	100	100	99
Inpainting	C1CC1	1	77	100	97
	C1CCC1	1	97	100	97
	c1ccccc1	1	39	100	100
	C1CCCCC1	1	95	93.68	100
ControlMol	C1CC1	99	97	100	88
	C1CCC1	99	97	96.91	95
	c1ccccc1	0	-	-	-
	C1CCCCC1	99	100	83	100

Table 3: Performance metrics on QM9 (without H). For each experiment, we randomly sample 100 molecules with fixed 9 atoms. Digress-Origin is the unconditioned base model we use.

Method	substructure	% condition ↑	% Valid ↑	% Unique over valid ↑	% connectivity ↑
Digress-Origin	-	-	72	100	99
Inpainting	C1CC1	100	43	100	98
	C1CCC1	100	26	100	97
	c1ccccc1	100	49	100	99
	C1CCCCC1	100	23	100	98
Repaint5	C1CC1	100	45	100	100
	C1CCC1	100	36	100	100
	c1ccccc1	100	62	100	100
	C1CCCCC1	100	36	100	100
Repaint20	C1CC1	100	66	100	97
	C1CCC1	100	43	100	97
	c1ccccc1	100	**76**	100	100
	C1CCCCC1	100	45	100	100
ControlMol	C1CC1	85	**84**	100	97
	C1CCC1	81	**80**	100	94
	c1ccccc1	100	73	100	97
	C1CCCCC1	100	**80**	100	98

Table 4: Performance metrics on MOSES. For each experiment, we randomly sample 100 molecules with fixed 26 atoms. Digress-Origin is the unconditioned base model we use.

valid 3D-conditioned molecules and has more relaxed requirements for datasets compared to other methods. We also get considerable results in Digress [Vignac *et al.*, 2022] and MiDi [Vignac *et al.*, 2023], which means it is likely to apply to other models in molecule science.

Our method does have some limitations, we replicate all layers of the base model, which results in the model requiring a quite larger GPU memory, especially when we try to extend our experiments to DRUGS [Axelrod and Gómez-Bombarelli, 2022] dataset (atoms number is up to 181), it's hard to train and work. So how to more effectively add additional module training and apply similar ideas to more applications in molecule science, may need to be explored in future work.

References

[Axelrod and Gómez-Bombarelli, 2022] Simon Axelrod and Rafael Gómez-Bombarelli. Geom, energy-annotated molecular conformations for property prediction and molecular generation. *Scientific Data*, 9, 2022.

[Böhm *et al.*, 2004] Hans-Joachim Böhm, Alexander Flohr, and Martin Stahl. Scaffold hopping. *Drug discovery today. Technologies*, 1 3:217–24, 2004.

[Dhariwal and Nichol, 2021] Prafulla Dhariwal and Alex Nichol. Diffusion models beat gans on image synthesis. *ArXiv*, abs/2105.05233, 2021.

[Dwivedi and Bresson, 2020] Vijay Prakash Dwivedi and Xavier Bresson. A generalization of transformer networks to graphs. *ArXiv*, abs/2012.09699, 2020.

[Erlanson *et al.*, 2016] Daniel A. Erlanson, Stephen W. Fesik, Roderick E. Hubbard, Wolfgang Jahnke, and Harren Jhoti. Twenty years on: the impact of fragments on drug discovery. *Nature Reviews Drug Discovery*, 15:605–619, 2016.

[Gebauer *et al.*, 2019] Niklas W. A. Gebauer, Michael Gastegger, and Kristof T. Schütt. Symmetry-adapted generation of 3d point sets for the targeted discovery of molecules. In *Neural Information Processing Systems*, 2019.

[Ho *et al.*, 2020] Jonathan Ho, Ajay Jain, and P. Abbeel. Denoising diffusion probabilistic models. *ArXiv*, abs/2006.11239, 2020.

[Ho, 2022] Jonathan Ho. Classifier-free diffusion guidance. *ArXiv*, abs/2207.12598, 2022.

[Hoogeboom *et al.*, 2021] Emiel Hoogeboom, Didrik Nielsen, Priyank Jaini, Patrick Forr'e, and Max Welling. Argmax flows and multinomial diffusion: Learning categorical distributions. In *Neural Information Processing Systems*, 2021.

[Hoogeboom *et al.*, 2022] Emiel Hoogeboom, Víctor Garcia Satorras, Clément Vignac, and Max Welling. Equivariant diffusion for molecule generation in 3D. In Kamalika Chaudhuri, Stefanie Jegelka, Le Song, Csaba Szepesvari, Gang Niu, and Sivan Sabato, editors, *Proceedings of the 39th International Conference on Machine Learning*, volume 162 of *Proceedings of Machine Learning Research*, pages 8867–8887. PMLR, 17–23 Jul 2022.

[Huang *et al.*, 2022] Lei Huang, Hengtong Zhang, Tingyang Xu, and Ka chun Wong. Mdm: Molecular diffusion model for 3d molecule generation. *ArXiv*, abs/2209.05710, 2022.

[Hughes *et al.*, 2011] Jp Hughes, Steven Rees, SB Kalindjian, and KL Philpott. Principles of early drug discovery. *British Journal of Pharmacology*, 162, 2011.

[Igashov *et al.*, 2022] Ilia Igashov, Hannes Stärk, Clément Vignac, Victor Garcia Satorras, Pascal Frossard, Max Welling, Michael M. Bronstein, and Bruno E. Correia. Equivariant 3d-conditional diffusion models for molecular linker design. *ArXiv*, abs/2210.05274, 2022.

[Jing *et al.*, 2022] Bowen Jing, Gabriele Corso, Jeffrey Chang, Regina Barzilay, and T. Jaakkola. Torsional diffusion for molecular conformer generation. *ArXiv*, abs/2206.01729, 2022.

[Kang and Cho, 2018] Seokho Kang and Kyunghyun Cho. Conditional molecular design with deep generative models. *Journal of chemical information and modeling*, 59 1:43–52, 2018.

[Li *et al.*, 2023] Yuheng Li, Haotian Liu, Qingyang Wu, Fangzhou Mu, Jianwei Yang, Jianfeng Gao, Chunyuan Li, and Yong Jae Lee. Gligen: Open-set grounded text-to-image generation. *2023 IEEE/CVF Conference on Computer Vision and Pattern Recognition (CVPR)*, pages 22511–22521, 2023.

[Lugmayr *et al.*, 2022] Andreas Lugmayr, Martin Danelljan, Andrés Romero, Fisher Yu, Radu Timofte, and Luc Van Gool. Repaint: Inpainting using denoising diffusion probabilistic models. *2022 IEEE/CVF Conference on Computer Vision and Pattern Recognition (CVPR)*, pages 11451–11461, 2022.

[Mou *et al.*, 2023] Chong Mou, Xintao Wang, Liangbin Xie, Jing Zhang, Zhongang Qi, Ying Shan, and Xiaohu Qie. T2i-adapter: Learning adapters to dig out more controllable ability for text-to-image diffusion models. *ArXiv*, abs/2302.08453, 2023.

[Polykovskiy *et al.*, 2018] Daniil Polykovskiy, Alexander Zhebrak, Benjamín Sánchez-Lengeling, Sergey Golovanov, Oktai Tatanov, Stanislav Belyaev, Rauf Kurbanov, Aleksey Anatolievich Artamonov, Vladimir Aladinskiy, Mark Veselov, Artur Kadurin, Sergey I. Nikolenko, Alán Aspuru-Guzik, and Alex Zhavoronkov. Molecular sets (moses): A benchmarking platform for molecular generation models. *Frontiers in Pharmacology*, 11, 2018.

[Rombach *et al.*, 2021] Robin Rombach, A. Blattmann, Dominik Lorenz, Patrick Esser, and Björn Ommer. High-resolution image synthesis with latent diffusion models. *2022 IEEE/CVF Conference on Computer Vision and Pattern Recognition (CVPR)*, pages 10674–10685, 2021.

[Ronneberger *et al.*, 2015] Olaf Ronneberger, Philipp Fischer, and Thomas Brox. U-net: Convolutional networks for biomedical image segmentation. *ArXiv*, abs/1505.04597, 2015.

[Satorras *et al.*, 2021a] Victor Garcia Satorras, Emiel Hoogeboom, Fabian B. Fuchs, Ingmar Posner, and Max Welling. E(n) equivariant normalizing flows. In *Neural Information Processing Systems*, 2021.

[Satorras *et al.*, 2021b] Victor Garcia Satorras, Emiel Hoogeboom, and Max Welling. E(n) equivariant graph neural networks. *ArXiv*, abs/2102.09844, 2021.

[Schneuing *et al.*, 2022] Arne Schneuing, Yuanqi Du, Charles Harris, Arian R. Jamasb, Ilia Igashov, Weitao Du, Tom L. Blundell, Pietro Li'o, Carla P. Gomes, Max Welling, Michael M. Bronstein, and Bruno E. Correia. Structure-based drug design with equivariant diffusion models. *ArXiv*, abs/2210.13695, 2022.

[Schütt *et al.*, 2017] Kristof Schütt, Pieter-Jan Kindermans, Huziel Enoc Sauceda Felix, Stefan Chmiela, Alexandre Tkatchenko, and Klaus-Robert Müller. Schnet: A continuous-filter convolutional neural network for modeling quantum interactions. In *Neural Information Processing Systems*, 2017.

[Sheynin *et al.*, 2023] Shelly Sheynin, Adam Polyak, Uriel Singer, Yuval Kirstain, Amit Zohar, Oron Ashual, Devi Parikh, and Yaniv Taigman. Emu edit: Precise image editing via recognition and generation tasks. *ArXiv*, abs/2311.10089, 2023.

[Song *et al.*, 2020] Yang Song, Jascha Narain Sohl-Dickstein, Diederik P. Kingma, Abhishek Kumar, Stefano Ermon, and Ben Poole. Score-based generative modeling through stochastic differential equations. *ArXiv*, abs/2011.13456, 2020.

[Torge *et al.*, 2023] Jos Torge, Charles Harris, Simon V. Mathis, and Pietro Lio'. Diffhopp: A graph diffusion model for novel drug design via scaffold hopping. 2023.

[Vignac *et al.*, 2022] Clément Vignac, Igor Krawczuk, Antoine Siraudin, Bohan Wang, Volkan Cevher, and Pascal Frossard. Digress: Discrete denoising diffusion for graph generation. *ArXiv*, abs/2209.14734, 2022.

[Vignac *et al.*, 2023] Clément Vignac, Nagham Osman, Laura Toni, and Pascal Frossard. Midi: Mixed graph and 3d denoising diffusion for molecule generation. In *ECML/PKDD*, 2023.

[Virshup *et al.*, 2013] Aaron Virshup, Julia Contreras-García, Peter Wipf, Weitao Yang, and David N. Beratan. Stochastic voyages into uncharted chemical space produce a representative library of all possible drug-like compounds. *Journal of the American Chemical Society*, 135 19:7296–303, 2013.

[Xu *et al.*, 2022] Minkai Xu, Lantao Yu, Yang Song, Chence Shi, Stefano Ermon, and Jian Tang. Geodiff: a geometric diffusion model for molecular conformation generation. *ArXiv*, abs/2203.02923, 2022.

[Yang *et al.*, 2023] Minjian Yang, Hanyu Sun, Xue Liu, Xi Xue, Yafeng Deng, and Xiaojian Wang. Cmgn: a conditional molecular generation net to design target-specific molecules with desired properties. *Briefings in bioinformatics*, 2023.

[Zhang *et al.*, 2023] Lvmin Zhang, Anyi Rao, and Maneesh Agrawala. Adding conditional control to text-to-image diffusion models, 2023.